

# PARTICLE CONFINEMENT AND TRANSPORT IN JT-60U

H. TAKENAGA, K. NAGASHIMA, A. SAKASAI, N. ASAKURA, K. SHIMIZU,  
H. KUBO, S. HIGASHIJIMA, T. OIKAWA, T. FUJITA, Y. KAMADA, N. HOSOGANE,  
M. SHIMADA AND THE JT-60 TEAM

Japan Atomic Energy Research Institute, Naka Fusion Research Establishment  
Naka-machi, Naka-gun, Ibaraki-ken, 311-0193, Japan

## Abstract

Particle confinement and transport have been systematically analyzed for the improved confinement modes in JT-60U. A scaling law for the total number of ions in the main plasma of ELMy H-mode plasmas was proposed for the first time with confinement times of the particles supplied by NBI (center fuelling) and by recycling and gas-puffing (edge fuelling) separately defined. The confinement time increases and decreases with density for center and edge fuelling, respectively. The comparison between the experimental data and the scaling was made for the high  $p$  ELMy H-mode and reversed shear plasmas. The particle confinement was enhanced over the scaling by a factor of about 2 in the reversed shear plasma. The particle diffusivity and convection velocity were also evaluated based on the perturbation technique using modulated helium gas-puffing in ELMy H-mode and reversed shear plasmas. The particle diffusivity and convection velocity were estimated to be 0.4-2 m<sup>2</sup>/s and -5.5 (inward)~+2.5 (outward) m/s for the ELMy H-mode plasma and to be 0.2-2 m<sup>2</sup>/s and -4 (inward)~0 m/s for the reversed shear plasma, respectively. The particle diffusivity was reduced by a factor of 5-6 around the internal transport barrier compared with that in the outside and inside regions in the reversed shear plasma.

## 1. INTRODUCTION

Density controllability is required in a fusion reactor for control of fusion power, for which understanding of particle confinement is essential. In NBI heated plasmas, particles are fuelled not only in the central region by NBI but also in the edge region by recycling and gas-puffing. Since the center and edge fuelled particles exhibit different confinement times [1], the particle confinement taking account of the effect of particle source distribution should be investigated. Furthermore, it is important to estimate the local particle transport coefficients for understanding of physical mechanism responsible for the particle confinement.

In this paper, confinement times for the particles fuelled by NBI and by recycling and gas-puffing were separately defined, and a scaling law for the total number of ions inside the separatrix was proposed for the ELMy H-mode plasmas. The scaling was systematically compared with experimental data for the high  $p$  ELMy H-mode and reversed shear plasmas. Furthermore, the particle transport coefficients were estimated based on perturbation technique using a modulated gas-puffing in the ELMy H-mode and reversed shear plasmas.

## 2. PARTICLE CONFINEMENT

In the steady state, the total number of ions ( $N_i$ ) inside the separatrix can be expressed as follows using the confinement times for particles fuelled by recycling and gas-puffing ( $\tau_p^R$ ) and for particles fuelled by NBI ( $\tau_p^{NB}$ ),

$$N_i = \tau_p^R (S_R + S_{GP}) + \tau_p^{NB} S_{NB} \quad (1)$$

where  $S_R$ ,  $S_{GP}$  and  $S_{NB}$  are the particle sources due to recycling, gas-puffing and NBI, respectively. The value of  $N_i$  was derived from the electron density and  $Z_{eff}$ . The value of  $S_R$  was estimated from D emission intensity. A large fraction of the recycling neutral particles ionizes in the divertor and scrape-off layer (SOL) in JT-60U [2]. The penetration probability of the neutral particles into the main plasma decreases from about 10% to a few % with increasing the main plasma density ( $2-3 \times 10^{19}$  m<sup>-3</sup>). Since the particle source in the divertor and SOL region largely contributes to the main plasma density [3],  $\tau_p^R$  was defined as the particle confinement time including the divertor and SOL, which means that the value of  $S_R$  used in this analysis includes the particle source in the divertor and SOL.

We derived a scaling law based on the data-set from ELMy H-mode plasmas with the plasma current ( $I_p$ ) of 1.0-1.8 MA, the toroidal magnetic field ( $B_T$ ) of 2.1-3.5 T, the absolute input power ( $P_{abs}$ ) of 5-25 MW, the line averaged electron density ( $\bar{n}_e$ ) of  $1-6 \times 10^{19}$  m<sup>-3</sup>, the plasma volume ( $V_p$ ) of 53-70 m<sup>3</sup>, the triangularity ( $\delta$ ) of 0.1-0.35 and  $Z_{eff} = 1.8-3.5$ . The dependence of  $\tau_p^R$  and  $\tau_p^{NB}$  on  $n_e$ ,

$$I_p, B_T \text{ and } P_{\text{abs}}^{\text{R}} \text{ was assumed as follows,} \\ \tau_p^{\text{R}} = \tau_p^{\text{R}}(0)(\bar{n}_e/1 \times 10^{19} \text{ m}^{-3}) (I_p/1 \text{ MA}) (B_T/3.5 \text{ T}) (P_{\text{abs}}/10 \text{ MW}), \quad (2)$$

$$\tau_p^{\text{NB}} = \tau_p^{\text{NB}}(0)(\bar{n}_e/1 \times 10^{19} \text{ m}^{-3}) (I_p/1 \text{ MA}) (B_T/3.5 \text{ T}) (P_{\text{abs}}/10 \text{ MW}). \quad (3)$$

We assumed that the dependence on  $I_p$ ,  $B_T$  and  $P_{\text{abs}}$  are the same for  $\tau_p^{\text{R}}$  and  $\tau_p^{\text{NB}}$ . From the fitting on the above assumption, the values of  $\tau_p^{\text{R}}(0)=4.7 \text{ ms}$ ,  $\tau_p^{\text{NB}}(0)=380 \text{ ms}$ ,  $\alpha^{\text{R}}=-0.36$ ,  $\alpha^{\text{NB}}=0.66$ ,  $\beta^{\text{R}}=0.21$ ,  $\beta^{\text{NB}}=0.26$ ,  $\gamma^{\text{R}}=-1.1$  were obtained. In Fig. 1, closed circles show the comparison between scaling and experimental data. The error bar in this figure is ascribed to uncertainties in  $Z_{\text{eff}}$ . It can be seen from this figure that the experimental data are well fitted to the scaling law. It is noted that the dependence of  $\tau_p^{\text{R}}$  on  $\bar{n}_e$  is different from that of  $\tau_p^{\text{NB}}$ . The decrease in  $\tau_p^{\text{R}}$  with increasing  $\bar{n}_e$  can be explained by localization of the particle source in the edge region including divertor and SOL with increasing  $\bar{n}_e$  [4]. The increase in  $\tau_p^{\text{NB}}$  with  $\bar{n}_e$  reflects the characteristics of plasma core confinement. The confinement times increase with  $I_p$  and  $B_T$ , and decrease with  $P_{\text{abs}}$ , which is similar as the dependence of the energy confinement time in the ELM-free H-mode plasma. The small ratio of  $\tau_p^{\text{R}}(0)/\tau_p^{\text{NB}}(0)$  indicates that density control with gas-puffing is associated with a drastic change of the particle flux onto the divertor plate, suggesting that the center fuelling such as pellet is necessary for density control.

In Fig. 1, open circles and squares show the comparison between the experimental data and the scaling in the high  $\tau_p$  ELMy H-mode ( $I_p=0.8\text{-}2 \text{ MA}$ ,  $B_T=1.8\text{-}4 \text{ T}$ ,  $P_{\text{abs}}=11\text{-}22 \text{ MW}$ ,  $\bar{n}_e=2\text{-}3.5 \times 10^{19} \text{ m}^{-3}$ ,  $V_p=52\text{-}60 \text{ m}^3$ ,  $\alpha=0.15\text{-}0.5$  and  $Z_{\text{eff}}=2\text{-}3.5$ ) and reversed shear ( $I_p=1.5\text{-}2.6 \text{ MA}$ ,  $B_T=3.4\text{-}4.4 \text{ T}$ ,  $P_{\text{abs}}=11\text{-}16 \text{ MW}$ ,  $\bar{n}_e=1\text{-}3 \times 10^{19} \text{ m}^{-3}$ ,  $V_p=55\text{-}65 \text{ m}^3$ ,  $\alpha=0.06\text{-}0.3$  and  $Z_{\text{eff}}=2.5\text{-}3.5$ ) plasmas, respectively. For the reversed shear plasmas, data during non steady state phase were included in Fig.1. In non steady state phase, eq. (1) can be rewritten as,

$$N_i^{\text{R}} = \tau_p^{\text{R}} (S_{\text{R}} + S_{\text{GP}} - dN_i^{\text{R}}/dt) + \tau_p^{\text{NB}} (S_{\text{NB}} - dN_i^{\text{NB}}/dt) \quad (4)$$

where  $N_i^{\text{R}}$  and  $N_i^{\text{NB}}$  are the numbers of ions fuelled by recycling and gas-puffing and by NBI, respectively. Here,  $dN_i^{\text{NB}}/dt$  was assumed to be equal to  $dN_i^{\text{R}}/dt$  because of  $\tau_p^{\text{R}} \ll \tau_p^{\text{NB}}$ , therefore,  $dN_i^{\text{R}}/dt$  was assumed to be zero. The value of  $dN_i^{\text{R}}/dt$  was considered as in the range of  $dN_e/dt \sim N_i/N_e \times dN_e/dt$ . An enhancement of particle confinement is not observed in the high  $\tau_p$  ELMy H-mode plasma. In the reversed shear plasma, the particle confinement seems to exhibit different dependence. Some data suggest that particle confinement is enhanced over the scaling by a factor of about 2. The enhancement of particle confinement is similar as or greater than the enhancement of energy confinement over the  $0.85_E^{\text{ELM-free}}$  scaling. This enhancement is closely related with the particle transport, which is discussed in the next section.

### 3. PARTICLE TRANSPORT

Gas-puffing modulation experiments were performed for the reversed shear ( $I_p=1 \text{ MA}$ ,  $B_T=2.1 \text{ T}$ ,  $P_{\text{abs}}=7.3 \text{ MW}$ ,  $\bar{n}_e=2.5\text{-}3.0 \times 10^{19} \text{ m}^{-3}$ ) and ELMy H-mode ( $I_p=1 \text{ MA}$ ,  $B_T=2.1 \text{ T}$ ,  $P_{\text{abs}}=11.1 \text{ MW}$ ,  $\bar{n}_e=2.1\text{-}2.4 \times 10^{19} \text{ m}^{-3}$ ) plasmas. We used helium gas-puffing, because the helium ion density can be directly measured using CXRS at 8 radial positions. The helium gas-puffing was modulated at 2 Hz. The electron density profiles for the reversed shear and ELMy H-mode plasmas are shown in Fig 2. An internal transport barrier (ITB) was observed in the region of  $r/a=0.4\text{-}0.5$  for the reversed shear plasma. The H-factor (enhancement factor above the ITER89-P scaling law) was estimated to be 1.9 and 1.3-1.5 for the reversed shear and ELMy H-mode plasmas, respectively. ELM activities were also observed in the reversed shear plasma.

The particle transport equations for the fully ionized helium ( $\text{He}^{2+}$ ) can be represented as follows:

$$\frac{dn_{\text{He}^{2+}}}{dt} = - \text{He}^{2+} + s_{\text{He}^{2+}}, \quad (5)$$

$$\text{He}^{2+} = -D \nabla n_{\text{He}^{2+}} + v n_{\text{He}^{2+}}, \quad (6)$$

where  $n_{\text{He}^{2+}}$  is the fully ionized helium density,  $\text{He}^{2+}$  is the helium ion flux density across the magnetic field,  $s_{\text{He}^{2+}}$  is the helium ion source density,  $D$  is the particle diffusivity and  $v$  is the convection velocity. Because helium was fuelled by gas-puffing only,  $s_{\text{He}^{2+}}$  is negligible in the region of  $r/a < 0.9$  with JT-60U plasma parameters. When we express the modulated helium ion density ( $\tilde{n}_{\text{He}^{2+}}$ ) as follows:

$$\tilde{n}_{\text{He}^{2+}} = A(r) \sin(\omega t - kr), \quad (7)$$

the time independent solution of  $D$  and  $v$  can be obtained as follows [5]:

$$D = - \left( Y \sin \theta + X \cos \theta \right) / r - A, \quad (8)$$

$$v = - \left( \left( \frac{A}{r} Y - \frac{A}{r} X \right) \sin \theta + \left( -\frac{A}{r} Y + \frac{A}{r} X \right) \cos \theta \right) / r - A^2, \quad (9)$$

where

$$X = \int_0^r r A \cos \theta dr \text{ and } Y = \int_0^r r A \sin \theta dr.$$

The helium transport was analyzed in ref. [6] for the reversed shear plasma of JT-60U based on the time response of the helium density profile to a short helium gas-puffing. In the analysis method used in ref. [6], the back ground helium ion density and the uncertainty in the source term affect the analysis results. The perturbation technique method used in this paper has advantages that the back ground helium ion density and the source term do not affect the analysis, and also a unique solution of the particle transport coefficients is obtained from the amplitude and phase profiles of the modulated helium density.

We fitted the helium ion densities measured by CXRS using a sum of sine and polynomial functions by the least squares fit method. The sine function expresses the modulated component and the polynomial function expresses the time evolution of the non-modulated component. In Figs. 3 (a) and (b), the amplitude and phase of the modulated helium ion density are plotted, respectively. The amplitude is similar for both cases in the region of  $r/a=0.1-0.3$  and  $0.7-0.9$ . However, the amplitude of the reversed shear plasma is smaller than that of the ELMy H-mode plasma in the region of  $r/a=0.3-0.7$ . The phase changed continuously for the ELMy H-mode plasma. In contrast, the phase changed significantly at the ITB region for the reversed shear plasma. The particle diffusivity and convection velocity were shown in Figs. 4 (a) and (b), respectively. Here, the profiles of the amplitude and phase of the modulated helium ion density as shown by the solid and dashed lines in Fig. 3 were used. The particle diffusivity was in the range of  $0.2-2$  and  $0.4-2$   $\text{m}^2/\text{s}$  for the reversed shear and ELMy H-mode plasmas, respectively. It can be seen from Fig. 4 (a) that the particle diffusivity was reduced in the reversed shear plasma by a factor of 5-6 in the ITB region compared with that in the inside and outside regions. In this discharge, the thermal ion diffusivity was estimated to be about  $0.3$   $\text{m}^2/\text{s}$  in the ITB region, which is almost the same as the particle diffusivity. In the region outside ITB, the particle diffusivity for the reversed shear plasma is also smaller than that for the ELMy H-mode plasma. This might be related to the fact that the heating power in the reversed shear plasma is smaller than that in the ELMy H-mode plasma. The inward pinch velocity of  $-2 \sim -1$   $\text{m/s}$  was observed in the ITB region for the reversed shear plasma. However, the increase of the inward pinch velocity in the ITB region was not observed. The inward pinch velocity was observed for the ELMy H-mode plasma except for the region of  $r/a=0.3-0.45$  as well as for the reversed shear plasma. The outward velocity could be related with the sawtooth activities. In this discharge, the sawtooth activities were observed and the inverse radius was evaluated to be  $0.3-0.4$ , which is the same as the outward velocity region.

These results show that the reduction of the particle diffusivity largely contributes to the enhancement of particle confinement for the reversed shear plasma. Since NBI source can penetrate to the region inside ITB,  $n_p^{\text{NB}}$  is enhanced by the reduction of the particle diffusivity. The inward pinch velocity and reduction of the particle diffusivity in the ITB region suggests that not only  $n_p^{\text{NB}}$  but also  $n_p^{\text{R}}$  are enhanced, because  $n_i/n_e$  is equal to  $v/D$  in the steady state in the region where the particle source is negligible.

#### 4. SUMMARY

The particle confinement and transport in JT-60U have been systematically analyzed. A scaling law for the total number of ions in the main plasma of ELMy H-mode plasmas is proposed. The particle confinement time increases and decreases with density for center and edge fuelling, respectively. In order to determine the dependence on other parameters such as plasma size and configuration, a data base has to be accumulated for many machines. In the reversed shear plasma, the particle confinement was enhanced by a factor of about 2 compared with the scaling. The particle diffusivity and convection velocity were estimated to be  $0.2-2$   $\text{m}^2/\text{s}$  and  $-4$  (inward) $\sim 0$   $\text{m/s}$  for the reversed shear plasma and to be  $0.4-2$   $\text{m}^2/\text{s}$  and  $-5.5$  (inward) $\sim 2.5$  (outward)  $\text{m/s}$  for the ELMy H-mode plasma, respectively. The particle diffusivity around the internal transport barrier was reduced by a factor of 5-6 compared with that in the inside and outside regions in the reversed shear plasma. The reduction of the particle diffusivity and the inward pinch velocity in the ITB region suggests that both particle confinement times of the center and edge fuelled particles are enhanced.

## REFERENCES

- [1] TAKENAGA, H., et. al., J. Nucl. Mater. 241-243 (1997) 569.
- [2] ASAKURA, N., et. al., to be published in J. Nucl. Mater.
- [3] TAKENAGA, H., et. al., Nucl. Fusion 37 (1997) 1295.
- [4] WOOTTON, A. J., et. al., Plasma Phys. Contr. Fusion 30 (1988) 1479.
- [5] TAKENAGA, H., et. al., Plasma Phys. Contr. Fusion 40 (1998) 183.
- [6] SAKASAI, A., et. al., Proc. of the 16th Int. Conf. on Fusion Energy (Montreal, 1996), IAEA, Vienna, Vol. 1 (1997) 789.

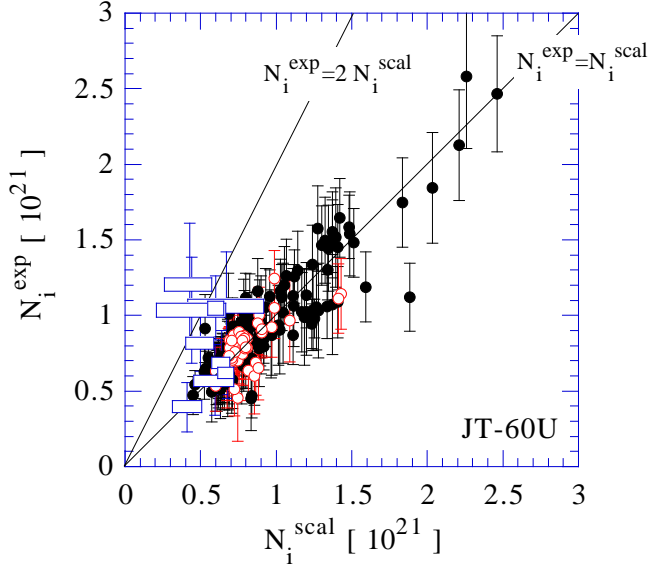


FIG. 1 Comparison between experimental total number of ions and its scaling. Closed circles, open circles and squares show the data for ELMY H-mode, high  $p$  ELMY H-mode and reversed shear plasmas, respectively.

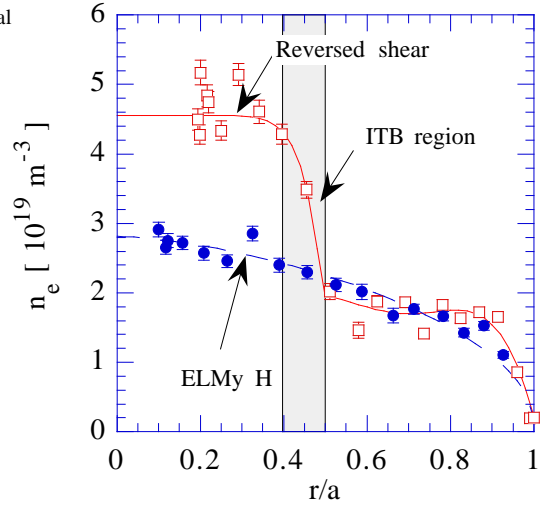


FIG. 2 Electron density profiles in the gas-puffing modulation experiments. Open squares and closed circles show the data for reversed shear and ELMY H-mode plasmas, respectively.

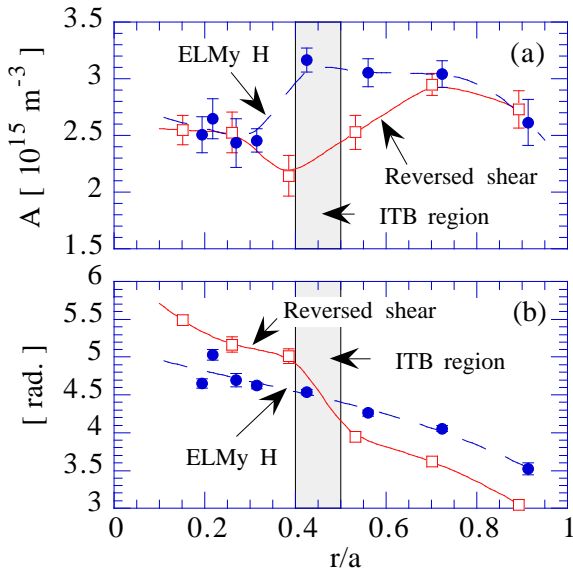


FIG. 3 Profiles of (a) amplitude and (b) phase of the modulated helium ion density. Open squares and closed circles show the data for reversed shear and ELMY H-mode plasmas. Solid and dashed lines show the fitting for reversed shear and ELMY H-mode plasmas, respectively.

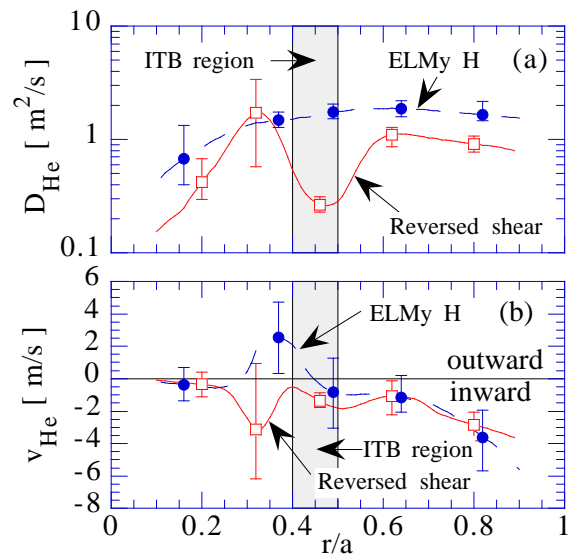


FIG. 4 (a) Particle diffusivity and (b) convection velocity profiles. Solid and dashed lines show the data for reversed shear and ELMY H-mode plasmas.